



Numerical Evaluation of Solar Power Potential for Off-Grid Applications in Rural Areas

Stephen A. Ajah^{1,2*}, Uchenna C. Nwokenkwo¹, O. Ezurike Benjamin¹, Samuel Uzoma Nwigwe¹, Chibuzo V. Ikwuagwu³, Friday N. Ashibong¹

¹Department of Mechanical/Mechatronic Engineering, Alex Ekwueme Federal University Ndufu-Alike Ikwo, Ebonyi State, Nigeria

²Applied Renewable & Sustainable Energy Research Group, Department of Mechanical Engineering, University of Nigeria, Nsukka 410001, Nigeria.

³Mechanical Engineering Department, University of Nigeria, Nsukka, Enugu State, Nigeria.

Received 29 Aug 2020,
Revised 29 Nov 2020,
Accepted 01 Dec 2020

Keywords

- ✓ Extraterrestrial,
- ✓ Solar Angle,
- ✓ Transmittance,
- ✓ Solar constant,
- ✓ Clear-sky.

stephen.aroh@funai.edu.ng
Phone: +2348063194697;
Fax: +2347067600735

Abstract

This study examined the different models for solar radiation and energy prediction within rural areas and also, applicable to other places for different months/days of the year considering eleven day-hour (7th - 17th). Scilab software was used in solving the models and calculating the atmospheric transmittance, diffuse transmission coefficient, clear sky radiation, horizontal beam radiation, diffuse to extraterrestrial beam radiation ratio, daily clearness index and power for different days of the months and years considering the day light hour. The atmospheric transmittance was found to be increasing towards the midday period daily from morning period but it annually has its peak around the April and September. Extraterrestrial radiation, clear sky radiation, horizontal beam radiation had their peak as well around the midday period daily on gradual increment from morning and, clear sky radiation is the highest radiation experienced within the metropolis throughout the year, followed by the horizontal beam radiation while the standard clear day radiation was the least among these three main sky radiations. These findings would help organizations in solving the problem of mini off-grid renewable energy generation and importance in agricultural activities by using these models to predict solar radiation peak energy period. Using a panel of 1 m², the peak energetic and exergetic output power were found to be 1.1MW and 0.55MW respectively with their respective efficiencies 0.536% and 0.261%.

1. Introduction

The sun has undoubtedly been proven to be the main primary source of energy for the earth. On daily basis, the sun releases enormous amount of radiant energy to the solar system for both plant and animal (man inclusive) utilization. These radiation from the sun moves in the space in the form of electromagnetic waves. When solar radiation passes through the atmosphere, the solar intensity dropped because of the atmospheric shield of the earth [1, 2]. This is mostly caused by the scattering and absorption of air molecules, dust particles and aerosols in the atmosphere with the radiation received by the earth [3]. The rays are then partially reflected and absorbed by the atmosphere such that the solar radiations received by earth have some direct and some diffused form of the radiations [4]. The energy content of sun that is release to the earth on daily basis is quite enormous and it is referred to as *solar energy*. Despite the considerable distance between the sun and the earth (about 1.5×10^{11} m), the amount of solar energy reaching the earth is substantial and are also in continuous usage by man. The energy

from the sun is usually regarded as renewable energy since its daily consumption rate is much less than their generation/production rate. It has been affirmed that the earth surface interrupts the passage of high amount energy of approximately 180×10^6 GW annually from the sun [5]. Nevertheless, solar radiation still serves as the earth's natural source of energy as well as the global energy power since almost every other life directly or indirectly depend on it for their survival. There are other natural sources of energy like the geothermal heat flux generated within the earth interior, atmospheric terrestrial radioactivity and cosmic radiation but they are negligibly small when compared to solar radiation [6, 7]. Based on this, it has be established that other aspects of the earth energy generation and life are affected by the solar radiation [8].

At any given geographical location or region, the daily solar radiation received changes with time due to the orbital rotation of the earth. For any given time, the solar radiation also varies in space as result of the changes in the deviation of solar rays with respect to the longitude, latitude and altitude of a particular location of interest [9]. The earth orbit around the sun also play important role for solar radiation prediction as shown in Figure 1. It can be seen that the earth polar axis of rotation is usually tilted at a constant angle of 23.5° when taken its elliptical plane as a reference point and this angle is always maintained during its annual orbit around the earth. The earth polar axis is usually tilted either away from or towards the sun which results to changes in seasons of the year but this does not take place at the equinoxes (Autumnal equinox and vernal equinox).

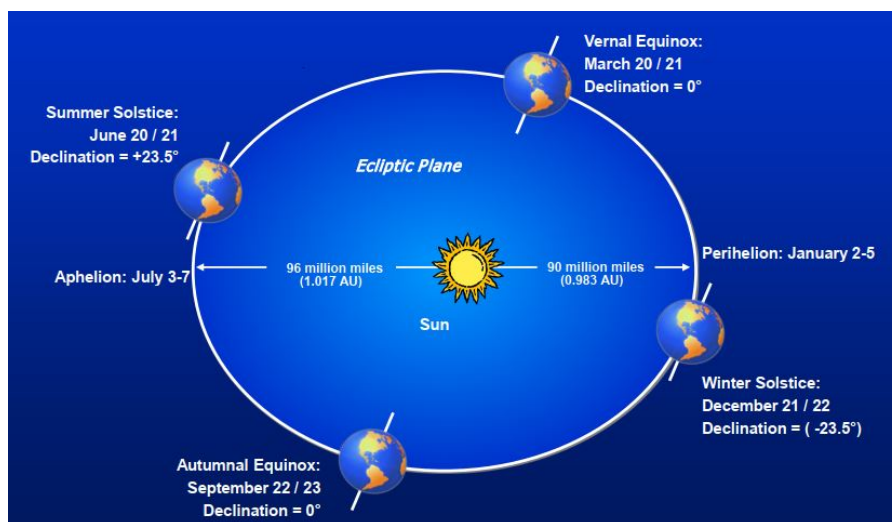


Figure 1: Earth's orbit around the sun [10]

In addition to the shielding effects of the cloud and other atmospheric constituents on the solar radiation intensities, the received intensities at any given location and time also depend on the relative position of the sun and the earth [11]. This is why the sun-earth orientation plays important role in prediction and determination of the received amount of solar radiation at any point in time. The earth's relative geometry to the sun can be described as a unique astronomical feature with its annual variation used in assessing the solar radiation data over certain period of time [6]. The solar time and the regional local time difference relative to the meridian can be attributed to the earth daily rotation about its imaginary pole called axis [9]. As earth rotates on its axis, it moves about 15° for every 1 hour (60 minutes) and completes a full circular rotation of 360° in 24 hours. The apparent cause of the solar angle deviation which also affects the intensity of the solar radiation can be related to some factors like the solar zenithal point, elevation and azimuthal angle though these angles are identical at the top of the equator since no change is introduced by the atmosphere itself [12]. The amount of solar radiation that

is trapped by the earth surface varies due to the variation in sun-earth orientation and also due to variation in daily spectral distribution as a result of atmospheric activities. As the earth slightly shift closer to the sun during its rotation, the solar irradiance impinging on a plane normal gets higher with respect to the sun rays [9, 13].

2. Application of solar energy generation

Solar energy usually serves as the vital renewable energy resources almost free to access apart from the installation cost and their installation as renewable energy technology has made energy generation more sustainable, pollution free, economical, highly reliable for longtime operation and secure energy source [14]. Although the major problem of Photovoltaic technology is its high capital costs compared to conventional energy sources, this aspect of technology should be adopted in remote areas to optimize the solar off grid potentials in combination with the other forms of renewable energies [15].

The high amount of energy requirement for daily activities and survival of human on earth cannot be overemphasize. The abundance of electrical energy is the central backbone of every developed economy in the world for life sustainability and technological advancement [16]. It can be said with utmost sincerity that no country can thrive without energy for any technological advancement and development for the well-being and comfort of the citizens. The underdevelopment, unemployment, political and economic crisis witnessed in Africa as a continent and Nigeria as a country still boil down to low power availability witnessed in the region. There is need for the country to seriously improve on power generation to combat these challenges and foster development in the region. There is also need for the energy generation approach to be environmentally friendly and sustainable to drastically reduce or possibly eliminate global warming and climate change which has been another challenge to the continent for decades now [17]. Solar energy is one of the generally accepted renewable and sustainable energy source globally and it is free in nature which is enormously needed by virtually all living being either directly or indirectly. Solar energy is highly environmentally friendly with almost no disadvantage in its usage and industrial applications. Solar energy research is not new research concept in Nigeria and has been gaining popular acceptance nationally and internationally [18]. Global solar radiation, extraterrestrial radiation and horizontal clear radiation estimations are very crucial in the prediction, evaluation or estimation of the possible solar energy generation in any particular or desired location. Mellit et al [19] developed a model with artificial neural network used to predict a daily global solar radiation data for voltaic power application which was validated with unspecified data. The prediction recorded mean relative error of 1.34% on the validation with high level of accuracy. Guessoum et al [20] have predicted the Algerian solar radiation data using RBF networks and the outcome of their solar radiation prediction model giving high accuracy 98.64%. Mohandes et al [21] did their own prediction using data from 41 recording stations in Saudi Arabia, the latitude, longitude, altitude and sunshine duration was used for the prediction of the mean monthly solar radiation and the results during the validation with the stations data resulted to 84% validity. Kalogirou et al [22] also employed recurrent neural network for the prediction of the maximum solar radiation from the environmental relative humidity and temperature with the obtained results showing correlation coefficient of about 98.58% and 98.75%. Standalone off-grid photovoltaic installation is shown in Figure 2. The standalone -grid system comprised of solar panels (arrays), controller, battery, inverter and household loads. The solar energy is trapped by the panels as a DC power. This passes through the controller to the inverter where is converted to AC power to consumption in appliances. The converted AC power is transferred to the residential building or other energy consumption units. The power can also be transferred to the battery for storage through the controller as shown in Figure 2.

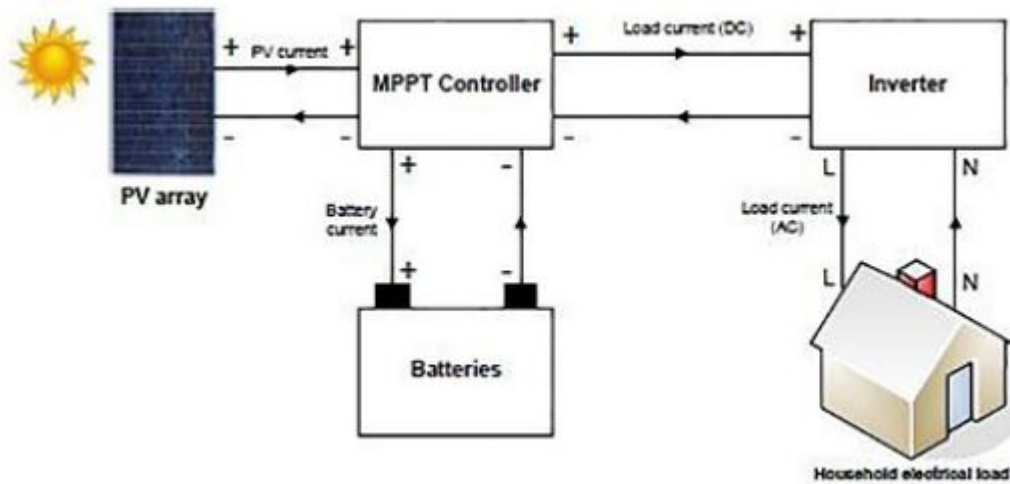


Figure 2: Sample of -grid photovoltaic installation [23]

The stored energy in the battery can be used later when the direct solar radiation is not available (usually in the night). For the past three decades, this energy systems technological set up had received interesting attention particularly in developing countries as government projects to overcome rural power challenges and as an affordable renewable energy sources. In the developed countries, this system can be integrated often with advanced fuel systems such as hydrogen energy technology [24]. Khan and Iqbal [25] in their studies investigated the technological feasibility of a hybrid system with hydrogen as an energy carrier in Newfoundland, Canada where they confirm that it's a promising and sustainable energy technology. Manirakiza et al [26] assessed the solar energy potential and wind energy potential in eastern region of Rwanda. In their study, the potential of wind energy and solar energy was determined and compared using the Rwanda Meteorological Agency data for the period from January 2016 to December 2017. The results indicated that the solar energy potential and wind energy potential are 280Wh m^{-2} per day and 1500Wh m^{-2} per day respectively. Chauhan and Saini [27] also presented residential energy management using off grid integrated renewable energy system for the remote areas of India. Micro hydro power (MHP), solar photovoltaic (SPV), wind, biomass were considered as the primary energy sources and battery as storage device to electrify the cluster of 12 villages of Dewal block of Uttarakhand state of India. They suggested demand side management (DSM) using load shift strategy for energy management. The comparative analysis with DSM and without DSM was presented and finally sensitivity analysis carried out for variation in biomass price, wind turbine cost and battery cost and performance of IRES was evaluated. Upadhyay and Sharma [28] developed hybrid energy system with cycle charging strategy for remote rural area in India. The hybrid energy system was developed using hydro, solar, biomass and biogas energy resources to satisfy the energy needs of 7 off-grid and non-electrified villages of Dhauladevi block of Almora district in Uttarakhand state of India. The developed model was optimized using particle swarm optimization (PSO) and genetic algorithm. Rajanna and Saini [29] proposed modelling of integrated renewable energy system considering solar, wind, micro hydropower, biomass and biogas energy sources for electrification of 26 off-grid villages of Chamarajanagar district of Karnataka state, India with no electricity access. In this context for some decades now, concentrating solar power plants (CSP) are getting increasing global attention for more efficient solar power generation. This technology has also helped to reduce carbon dioxide emissions in power generation sector and domestic based heat generation with climate change reduction [30, 31, 32]. The CSP plant technology is still far from the conventional power plants in the energy sector on which the actual costs and system performances usually don't have much discrepancies with the

projected value. More experience skilled operations has to be employed to properly develop and improve the technology for higher operating efficiencies. Thermal energy storage system usually plays a positive role in annual electricity generation and system capacity factor if seriously given technological attention [33]. Stephen [34] in his study found out that using renewable source such as wind or solar photovoltaic (PV), off-grid electric power systems can be generated with a back-up power provided by a propane fueled motor/generator. In this design, residential energy consumers had the option of employing an electric refrigerator with the normal vapor compression refrigeration system, or a fuel-fired refrigerator operating as an absorption refrigeration system. Other relevant works done on off grid rural power survey, generation and distribution can be gotten in some literature [35, 36, 37, 38, 39].

3. Analysis

3.1. Selected location for data collection

Obegu Aba around Abakaliki, the capital of Ebonyi State was considered as the study area of this research. Abakaliki in Ebonyi state as one the agriculturally based states in the country Nigeria with enormous potentials for harnessing solar energy was chosen for data computations used in this study. It is bounded by four states; Benue state (North), Enugu state (West), Abia (South), and Cross River state (East). Ebonyi state has the total land area of 5935km² which is approximately 593,500 hectares out of which 534,150 hectares is an arable fertile soil for agricultural cultivation [40]. Abakaliki is the capital city of Ebonyi state as one of the South Eastern states of Nigeria and it is located within the latitude of 6.32⁰N and longitude of 8.12⁰E with its altitude of approximately 118m. The city is always hot which is characterized with severe solar radiation intensity. It is therefore necessary to evaluate and predict the solar radiation within Abakaliki metropolis for its uses in energy (power) generation, solar drying of agricultural produce and other agricultural activities.

4. Solar radiation prediction models

Solar radiation study is a very interesting area of research. The variation of solar radiation intensity is a function of many variables (latitudinal location of the place of interest, longitudinal location of the place of interest, atmospheric transmittance for the beam radiation, air mass etc). The scattering and absorption of solar radiation as a result of the effects of the shielding atmospheric constituents varies with daily time because atmospheric conditions and air mass changes with daily time. It is very crucial to define a standard clear sky and calculate the hourly and daily radiation of the location which would be received on a horizontal surface under these standard conditions. The method of estimating the beam radiation transmitted through the atmospheric condition, taking zenith angle and altitude of the location into consideration is a crucial factor to be evaluated. Atmospheric transmittance $\tilde{\tau}_b$ as one the determining factors of the solar radiation is given by:

4.1. Atmospheric transmittance

$$\tilde{\tau}_b = a_0 + a_1 \exp\left(\frac{-k}{\cos\theta_z}\right) \quad (1)$$

The constants a_0 , a_1 and k for the standard atmosphere within some certain kilometers visibility are found from a_0^* , a_1^* and k^* which are given for altitudes less than 2.5km by

$$a_0^* = 0.4237 - 0.00821(6 - A)^2 \quad (2)$$

$$a_1^* = 0.5055 + 0.00595(6.5 - A)^2 \quad (3)$$

$$k^* = 0.2711 + 0.01858(2.5 - A)^2 \quad (4)$$

where A is the altitude of the location from an observer in kilometers. Correction factors are applied to a_0^* , a_1^* and k^* are to be used to allow for changes in climate types. The correction factors are:

$$r_0 = \frac{a_0}{a_0^*}, r_1 = \frac{a_1}{a_1^*} \text{ and } k_k = \frac{k}{k^*}$$

For tropical region like that of Abakaliki, Nigeria; $r_0 = 0.95$; $r_1 = 0.98$ and $r_k = 1.02$.

$$\cos\theta_z = \cos\phi\cos\delta\cos\tilde{\omega} + \sin\phi\sin\delta \quad (5)$$

The variable ϕ is the latitude of the location north or south of the equator. $\tilde{\omega}$ is the hour angle of the sun east or west of the local meridian due to rotation of the earth. To determine the hour angle $\tilde{\omega}$ for a any time of the day, 15° angular rotation from the earth's axis is equal to an hour time change. Morning hours change are taken to be negative from 12 noon (as a reference point of 0°) while afternoon hours are taken to be positive. This is given by

$$\tilde{\omega} = 15(T_m - 12) \quad (6)$$

where T_m is the local time of the location of interest in daily hour. δ is the declination which is the angular position of the sun at solar noon (i.e., when the sun is on the local meridian) with respect to the plane of the equator and it is given by

$$\delta = 23.45 \sin\left(360 * \frac{284 + n}{365}\right) \quad (7)$$

n is the number of days in the year for the particular day of interest taking for example January 1st as number 1 which can be found from table [Table 1](#).

Table1: Days for months and values of n by the months

Months	n(ith day in Months)	n(average day in Months)	monthly date	Declination
January	n	17	17	-20.9 ⁰
February	31+n	47	16	-13 ⁰
March	59+n	75	16	-2.4 ⁰
April	90+n	105	15	9.4 ⁰
May	120+n	135	15	18.8 ⁰
June	151+n	162	11	23.1 ⁰
July	181+n	198	17	21.2 ⁰
August	212+n	228	16	13.5 ⁰
September	243+n	258	15	2.2 ⁰
October	273+n	288	15	-9.6 ⁰
November	304+n	318	14	-18.9 ⁰
December	334+n	344	10	-23 ⁰

4.2. Beam radiations

The transmittance for the case of standard clear radiation and beam radiation can be determined for any zenith angle and any altitude up to 2500m. The clear-sky beam radiation I_{cnb} is then given by

$$I_{cnb} = I_{cnb} \tilde{\tau}_b \quad (8)$$

To determine the extraterrestrial radiation incident from universal solar constant I_{cs} , a dimensionless extraterrestrial factor f_r is expressed as

$$f_r = \left(1 + 0.033 \cos \frac{360n}{365}\right) \quad (9)$$

where I_{on} is the extraterrestrial radiation incident on the plane normal to the radiation on the n th day of the year.

$$I_{on} = I_{sc} f_r \quad (10)$$

where a universal solar constant of approximate value of 1367 W/m^2 was adopted for I_{sc} . The clear-sky horizontal beam radiation I_{cb} is expressed as a function of the extraterrestrial radiation I_{on} and it is given by:

$$I_{cb} = I_{on} \tilde{\tau}_b \cos \theta_z \quad (11)$$

4.3. Transmission coefficient

Liu and Jordan [41] has also generated an empirical model relating $\tilde{\tau}_b$ and τ_d as shown in Equation.12. The relationship was derived based on measured data from three stations and it was consistent on the validation process.

$$\tau_d = 0.271 - 0.294 \tilde{\tau}_b \quad (12)$$

It is necessary to relate the normal incident solar radiation to the universal solar constant to enhance its prediction. Usually, the solar radiation incident on a horizontal plane is the normal incident solar radiation I_o is given by:

$$I_o = I_{sc} f_r \cos \theta_z \quad (13)$$

4.4. Extraterrestrial radiation on surfaces

It is important to integrate daily extraterrestrial radiation on a horizontal surface H_o into daily incident solar radiation calculation. H_o the radiation that can be received in the absence of the atmospheric shielding and can be given as a function of total daily insolation, $I_{D,sc}$, I_{on} and $\theta_{z,tk}$.

$$I_{D,sc} = \frac{24 * 3600 I_{on}}{\pi} \quad (14)$$

where $\theta_{z,tk}$ known as solar angle tracking factor is given by:

$$\theta_{z,tk} = \cos \phi \cos \delta \sin \omega_s + \frac{\pi \omega_s}{180} \sin \phi \sin \delta \quad (15)$$

where ω_s is the sunset angle given by:

$$\omega_s = \frac{\sin \phi \sin \delta}{\cos \phi \cos \delta} \quad (16)$$

$$H_o = I_{D,sc} \theta_{z,tk} \quad (17)$$

Extraterrestrial radiation on a horizontal surface for a certain hour period \tilde{H}_o , can be calculated by integrating Equation 15 for a period between hour angles ω_1 and ω_2 to replace ω_s in the equation which define a certain hour (where ω_2 is the larger), resulting to Equation 18.

$$\tilde{H}_o = \frac{I_{D,sc}}{2} \theta_{z,htk} \quad (18)$$

where $\theta_{z,htk}$ is the hourly solar angle tracking factor is given by:

$$\theta_{z,htk} = \cos\phi\cos\delta(\sin\omega_2 - \sin\omega_1) + \frac{\pi(\omega_2 - \omega_1)}{180} \sin\phi\sin\delta \quad (19)$$

The sunrise hour angle is the negative of the sunset hour angle.

$$\omega_r = -\omega_s \quad (20)$$

It also follows that the number of daylight hours N is given by:

$$N = \frac{2}{15} \cos^{-1}\omega_s \quad (21)$$

5. The PV trapped energy

The term Photovoltaic (PV) is today the major technology used to convert solar radiation (sunlight) directly into electricity. The two terms that made up *photovoltaic* are *photo* which means **light** and *voltaic* which is **electricity**. A photovoltaic (PV) cell is most times in simple term refers to *solar cell*. This is made up of series of semiconductors which are capable of generating electricity when light strikes on them. When solar radiation strikes on a PV cell, the photons of the absorbed sunlight shift some of the electrons from the solar cell atoms. The free electrons then move through the cell, creating and at the same time filling some holes in the solar cell. This movement of electrons and holes develop different potential at different locations leading to certain level of potential difference in the panel resulting to electricity generation. This physical process through which a PV cell converts sunlight into electricity is known as the *photoelectric effect*. The PV module also have some operating controlling parameters which influence the output power. In this numerical study, a certain solar farm of total PV surface area (A_{pv}) of 2.25m² was used for the predictive study with the properties in Table 2. Markvart [42] has developed a model for predicting the PV operating temperature using the standard active cell operating temperature T_{OT} , the PV module operating temperature, $T_{c,ak}$ can be expressed in terms of the in-plane irradiance and other parameters as:

$$T_{c,ak} = T_a + \frac{I_{ir}}{I_{OT}} (T_{OT} - T_{a,OT}) \quad (22)$$

where T_a is the ambient temperature, I_{ir} is the in-plane irradiance and T_{OT} is the technology dependent on the nominal operating cell temperature, which is the cell temperature at its reduced operating irradiance $I_{OT} = 1\text{kW/m}^2$, the PV active cell operating temperature relative to the ambient temperature $T_{a,OT} = 20^\circ\text{C}$, T_{OT} depends on the PV technology and has a typical value of about 45°C . Based on the evaluation of the developed model by Duffie and Beckman [43] with Abakaliki climatic condition, the PV module operating temperature model is expressed as:

$$T_{c,ak} = 30 + 0.0175 (G_t - T_{a,OT}) + 1.1 (T_{md,ak} - T_r) \quad (23)$$

where $T_{md,ak}$ and T_r are the PV module mean operating temperature and the environmental reference temperature respectively.

Similarly, the PV tracking efficiency η_{Trk} can also be written as a function of the PV nominal efficiency:

$$\eta_{Trk} = \eta_n [1 - \beta_{TC} (T_{c,ak} - T_r)] \quad (24)$$

η_n is the PV nominal efficiency usually specified in the manufacturers' catalogue.

Table2: Different PV simulation parameters for the power estimation

Parameters	Description	Assumed numerical value	Units
A_{ab}	Location altitude	58.5	Km
T_r	Reference temperature	25 (above sea level)	$^{\circ}\text{C}$
A_{pv}	PV surface area	2.25	m^2
α_{pv}	PV absorptivity	0.04	
ρ_{pv}	PV reflectivity	0.05	
I_{sc}	solar constant	1.367	kW/m^2
η_n	PV nominal efficiency	0.3	17
$T_{md,ak}$	Location mean temperature	30	$^{\circ}\text{C}$
ϕ_{ab}	Location altitude	6.32	$^{\circ}\text{N}$

The fractional energy drop associated with Paker conditioning and miscellaneous losses E_{nff} can be expresses as:

$$E_{nff} = (1 - I_{mml})(1 - I_{pcl}) \quad (25)$$

I_{mml} is the miscellaneous module losses fraction while I_{pcl} is the fractional losses associated with power conditioning.

The average tracked clear sky horizontal beam radiation on the PV can be expressed as a function of the reflectivity and absorptivity of the PV material (α_{pv} and ρ_{pv} respectively) with respect to the mean clear horizontal beam radiation I_{cb} within the location of interest. The I_{cb} from Equation 11 can thus be written as:

$$I_{cb,m} = I_{cb}[1 - (\alpha_{pv} + \rho_{pv})] \quad (26)$$

The mean PV output power can then be evaluated from the parameters in Equations 23, 24, 25 and 26 as:

$$P_{exe,out} = A_{pv} * \eta_{Trk} * E_{nff} * I_{cb,m} \quad (27)$$

The output efficiency of the PV η_{pv} is define as the PV output power divided by the input solar power (solar radiation). Dividing Equation 27 by I_{sc} gives the output efficiency of the PV.

$$\eta_{pv} = \frac{P_{out}}{I_{sc}} \quad (28)$$

From the second law of thermodynamics, some of the generated power of the PV will be lost in the form of destroyed exergy during the process due to entropy generation in the system. Exergetic power of a system is equal to the maximum amount of power obtainable when the system is brought from its state to a dead state by processes during which the system may interact only with the environment [44]. Based on this, Equation 27 cannot be taken as the real output power from the system; hence, exergetic power output from the system can be stated as a function of the PV operating temperature and that of the reference temperature. The PV exergetic output power $P_{exe,out}$ is given by:

$$P_{exe,out} = P_{exe,out} \left(1 - \frac{T_r}{T_{c,ak}} \right) \quad (29)$$

The exergetic efficiency can also be expressed as the second law efficiency of the system. The exergetic efficiency which is the true system efficiency is stated PV exergetic power divided by the input solar exergetic power (solar exergy). Hence, PV exergetic efficiency $\eta_{exe,pv}$ can be expressed as:

$$\eta_{exe,pv} = \frac{P_{exe,out}}{I_{ex}} \quad (30)$$

$$I_{ex} = I_{sc} \psi \quad (31)$$

where Njoku et al [45], expressed ψ as:

$$\psi = 1 - \frac{4}{3} \left(\frac{T_r}{T_s} \right) + \frac{1}{3} \left(\frac{T_r}{T_s} \right)^4 \quad (32)$$

where T_s is the mean temperature of the sun.

6. Results and discussion

The above models and equations were solved using Scilab 6.0.2 software to calculate the beam radiations, radiation transmittance and the respective coefficients, day clear radiation, extraterrestrial radiation, etc. The data generated from the software after solving the above equations were equally plotted against the hours of the day N (as calculated from the formula above) from 7th hour (7:00am) to 17th hour (5:00pm) when the solar radiation is noticeable. Though sometimes in the year in the tropical region, the solar radiation may be noticeable but relatively very low beyond these aforementioned times. For the purpose of this work, the aforementioned time is taken as the active period to sensible solar radiation and transmittance in the day.

6.1. Annual transmittance and radiation variation for different hours of the day

We can see from [Figure 3](#) that the atmospheric transmittance has lowest values of 0.604 and 0.525 for 12:00pm and 9:00am respectively around January and December period where the two months are maintaining relatively equal transmittance. Around April and September period, there is appreciable increase in the transmittance to value of 0.631 and 0.560 for 12:00pm and 9:00am respectively since it is a function of several factors like the relative humidity, daily temperature readings and solar radiation intensity. Around the middle of the year, lower values of 0.622 and 0.551 for 12:00pm and 9:00am respectively were gotten even though the numerical difference is not much.

It was observed as well that the atmospheric transmittance around the midday is always higher than that of the morning hour period like 9:00am throughout the year. The extraterrestrial radiation plot can equally be seen in [Figure 3](#). It was at its peak (1413W/m^2) around the beginning and the end of the year. The minimum value of 1322W/m^2 was equally observed around the middle of the year due to the heavy rainy season and other factors witnessed during that period.

In [Figure 4](#), the 3D surface plot of the horizontal clear sky radiation can be seen. The horizontal clear sky radiation increases gradually from 150W/m^2 to its peak value of 790W/m^2 around the midday hour, thereafter dropped gradually to the initial value as the sun set approaches. Meanwhile, it maintains almost relatively higher value around the early and later part of the year but lower within the middle of the year through gradual decrease. This is as result of the serious dry and rainy season witness within the Abakaliki metropolis during the beginning/ending and the middle part of the year respectively. The

standard clear day radiation was also plotted to show its variation across the year. It can be shown that it recorded its maximum value of 115.8W/m^2 during the dry season of the year and as well its minimum value of 108.3W/m^2 was observed during the middle of the year as rainy season is witness during the period.

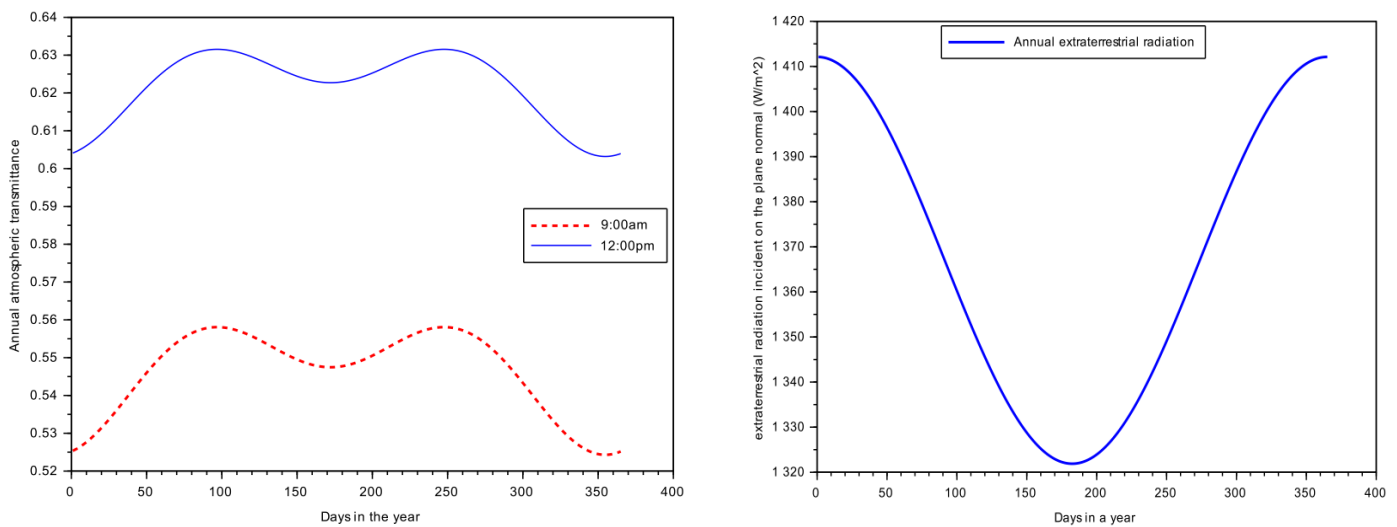


Figure 3: Annual atmospheric transmittance and extraterrestrial radiation

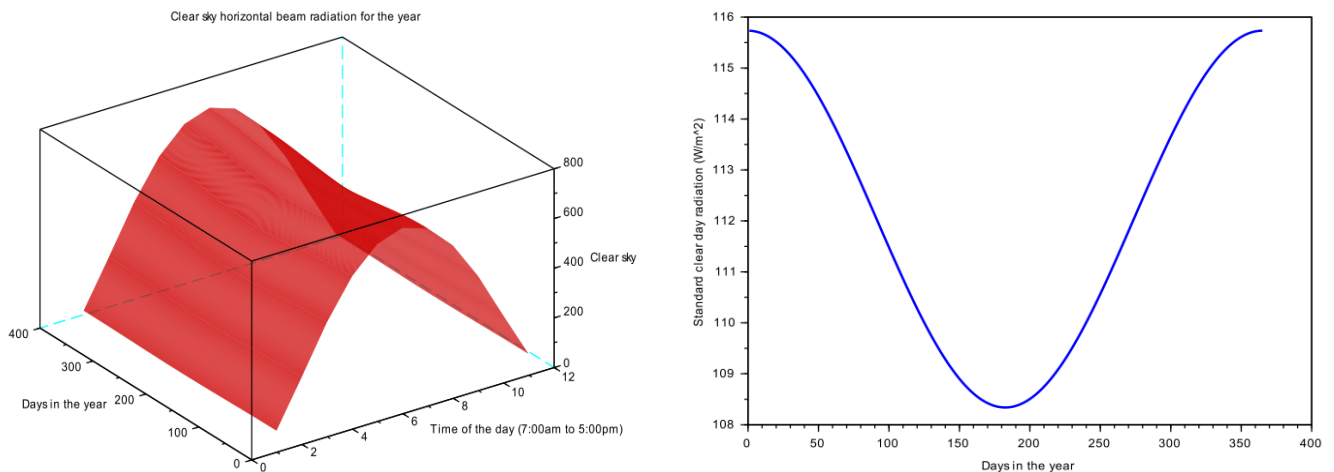


Figure 4: Annual horizontal clear sky and standard clear day radiation

In [Figure 5](#), the 3-D surface plot of the clear sky normal beam radiation can be seen. The clear sky normal beam radiation increases gradually from 320W/m^2 to its peak value of 850W/m^2 around the midday hour, thereafter dropped to the initial value towards the sun set hours. Meanwhile, it maintains almost relatively higher value around the early and later part of the year but lowers within the middle of the year through gradual decrease. This is as a result of the serious dry and rainy season usually witnessed within the Abakaliki metropolis during the beginning/end and the middle part of the year respectively. The diffused to extraterrestrial radiation ratio was also plotted to show its variation across the year. We can see from [Figure 5](#) that the diffused-to-extraterrestrial radiation ratio has the values 0.0954 and 0.1165 for 12:00pm and 9:00am respectively around January and December period where the two months are maintaining relatively equal diffused to extraterrestrial radiation ratio. Around April and September period, there is appreciable decrease in their values to 0.0851 and 0.107 for 12:00pm and 9:00am respectively. Around the middle of the year, slightly higher values of 0.0858 and 0.11 for 12:00pm and 9:00am respectively were recorded with little numerical difference.

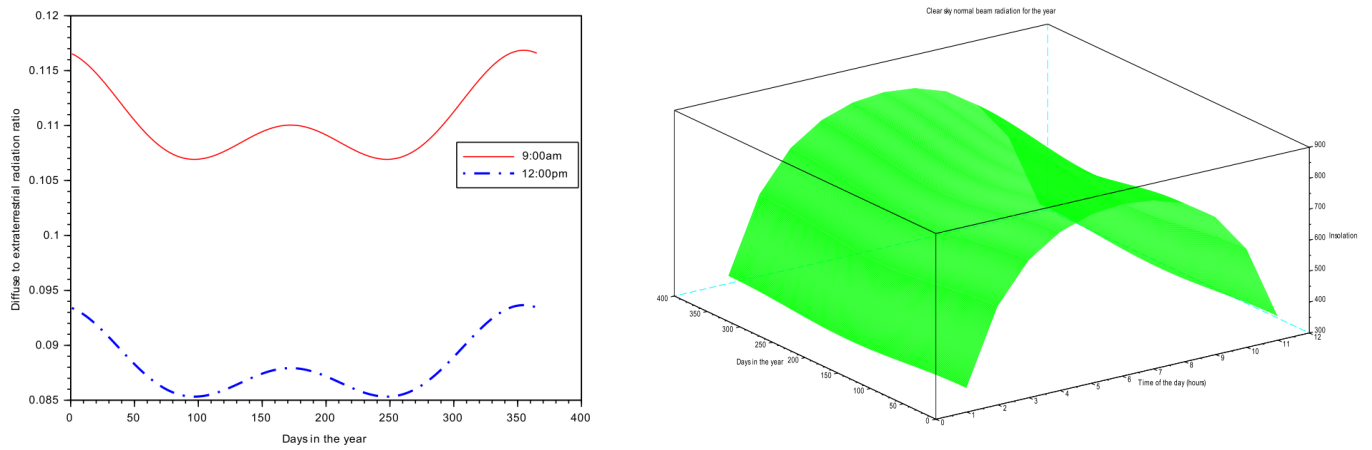


Figure 5: Annual clear sky normal beam and diffused to extraterrestrial radiation ratio

6.2. Monthly transmittance and radiations for different hours of the day

The average monthly data for different radiations and transmittance were computed for different hours of the day. As stated earlier, some selected months data were computed against the time of the day. [Figure 6](#) shows the plot of the horizontal clear sky radiation and diffuse to extraterrestrial beam radiation ratio for some selected months (January, February, April, September and December). It can be seen from the plot that the January and December data are relatively equal, same is applicable for April and September in line with the observation for the previous annual data plot. This observation is the same for both the horizontal clear sky radiation and diffuse to extraterrestrial beam radiation ratio as seen in [Figure 6](#). As the horizontal clear sky radiation increases gradually to its peak around the midday, the reverse is the case for diffuse to extraterrestrial beam radiation ratio as it decreases to its minimum value around the midday. This is because the extraterrestrial beam radiation is at its peak around the midday whereas the diffuse radiation is not. It can as well be observed that the April/September horizontal clear sky radiation is higher than that of January/December case because seasonal transition is usually witnessed around the April/September period resulting to clearer horizontal sky radiation.

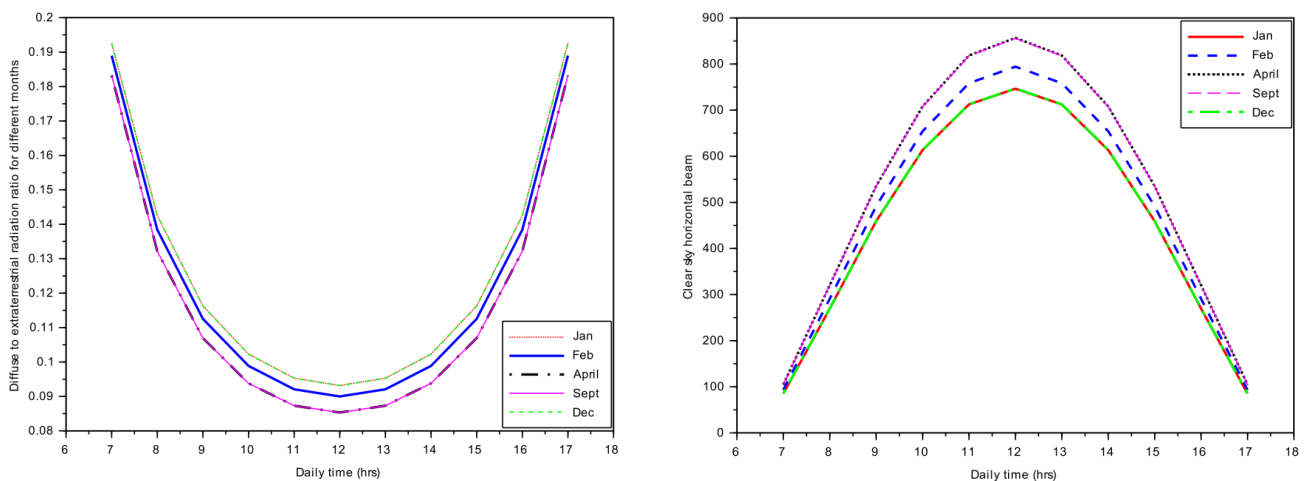


Figure 6: Diffuse to extraterrestrial beam radiation ratio and horizontal clear sky radiation for some selected months

The clear sky normal radiation, clear sky horizontal beam radiation and standard clear day radiation were plotted against the daily hours for different months of the year to determine their variation in the day. In [Figure 7](#), January plot for the three different radiations were shown as an example. Meanwhile, the clear sky normal radiation is greater (with the peak value of 850W/m^2) than the other two at any time of the day; this is followed by the clear sky horizontal beam radiation (with the peak value of 740W/m^2) while

the standard clear day radiation has the least (with the peak value of 110W/m^2) around the midday period. All gradually increase from morning period to their peak value during the midday when the sun is directly overhead north and the intensity is high. The daily clearness index was also computed and plotted for different months against the daily time of the day as shown in Figure 7. September has the highest clearness index of 0.85 followed by April; but December has the least clearness index with January and October slightly above that. This is as a result of the harmattan effect been experienced during those periods especially the December. April and September period always have higher clearness index since those periods are the seasonal transition periods in the year. Meanwhile, the index increases gradually from morning period to its peak around the midday time on the average day of month.

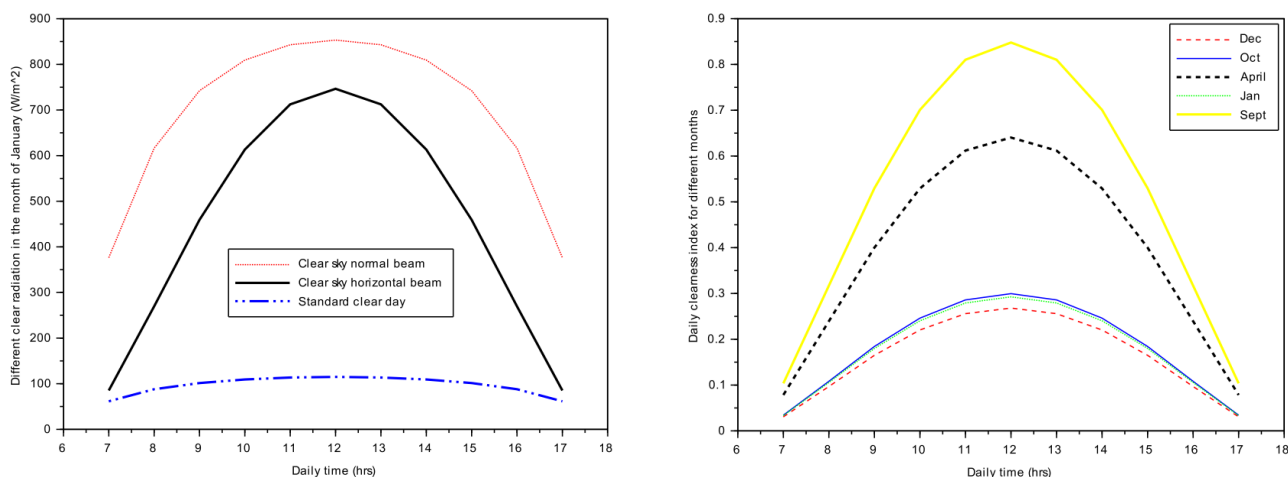


Figure 7: January radiation and the daily clearness index for different months

Annual clear sky radiation and standard clear day radiation for different days in the year were plotted against the different hours of the day. In Figure 8, the clear sky radiation was plotted against the 365 days in the year. It was discovered that the beginning and the end months of the year (January and December) witnessed had the peak value with the middle month having the least value across all the daily hours.

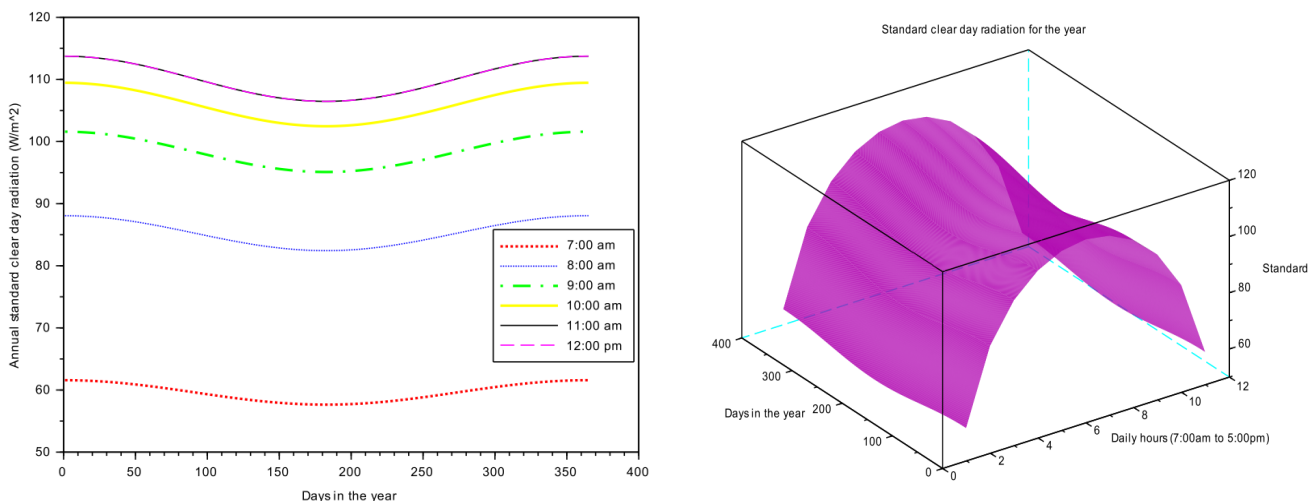


Figure 8: Annual clear sky and standard clear day radiation for different days in the year

For the 3D plot of the standard clear day radiation against the daily time and days of the year. The radiation gradually increases from its initial value of 58W/m^2 in the morning to 118.5W/m^2 in the midday when the solar angle has a value of 0° and the sun is at its peak. Again, the beginning and the end of the

months of the year (January and December) also had the peak standard clear day radiation with the middle of the year month (June) has the least value.

6.3. PV output power for different hours of the day

By solving Equation 27, Equation 28, Equation 29 and Equation 31 with Scilab software, the PV energetic power, 1st law efficiency, exergetic power and exergetic (2nd law) efficiency were respectively evaluated. Equations 23 – 26 were used as input variables in solving the above equations. Meanwhile, the peak power as well as efficiency were observed to occur around the midday when the solar radiation is always at the peak. From figure 9, it can be observed that the approximate peak energetic and exergetic power value of 1.1MW and 0.55MW respectively. Some selected days of some months were used for validation of these models. It can also be observed that January, December and November period recorded the peak value of power. This can be attributed to the intense high solar radiation and the high clear sky radiation been witnessed in the region during the said period. The July days recorded the least followed by April days due to cloudy conditions and intense rain do witnessed during the said period. January and December days can be seen to coincide in the plot because the atmospheric conditions of the two months are almost the same.

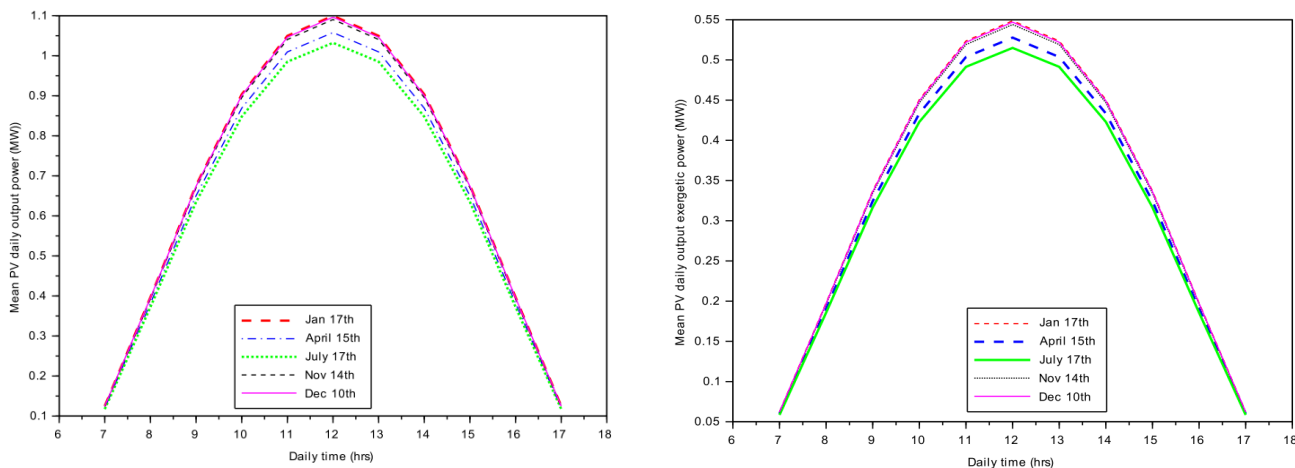


Figure 9: PV daily energetic and exergetic output power

The same trend is also maintained for the case of energetic and exergetic efficiencies with their respective peak values of 0.536% and 0.261% at the month of January. This low exergetic efficiency is due to other miscellaneous losses witnessed in the PV system in addition to shielding from dirt. This is shown in figure 10 with the energetic and exergetic efficiencies on the left and right side respectively.

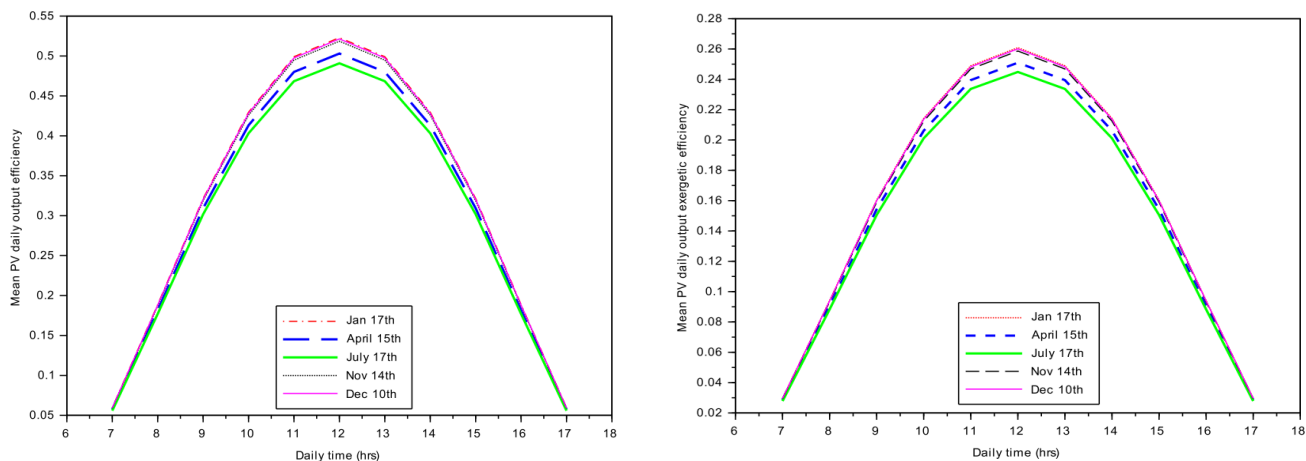


Figure 10: PV daily first law and second law efficiencies

Again, the two efficiencies relation is in line with that of the two different PV output power. Figure 11 shows the possibility of running one week (7 days) simulation of the PV system for a mini off grid power generation within a particular location (such as Abakaliki metropolis).

7. Summary

The different solar radiation models has been reviewed and studied for solar radiation prediction within Abakaliki metropolis for different months of the year considering 7th to 17th hour of the day. The altitude, latitude and longitudinal location of Abakaliki localities on global map was used for this study.

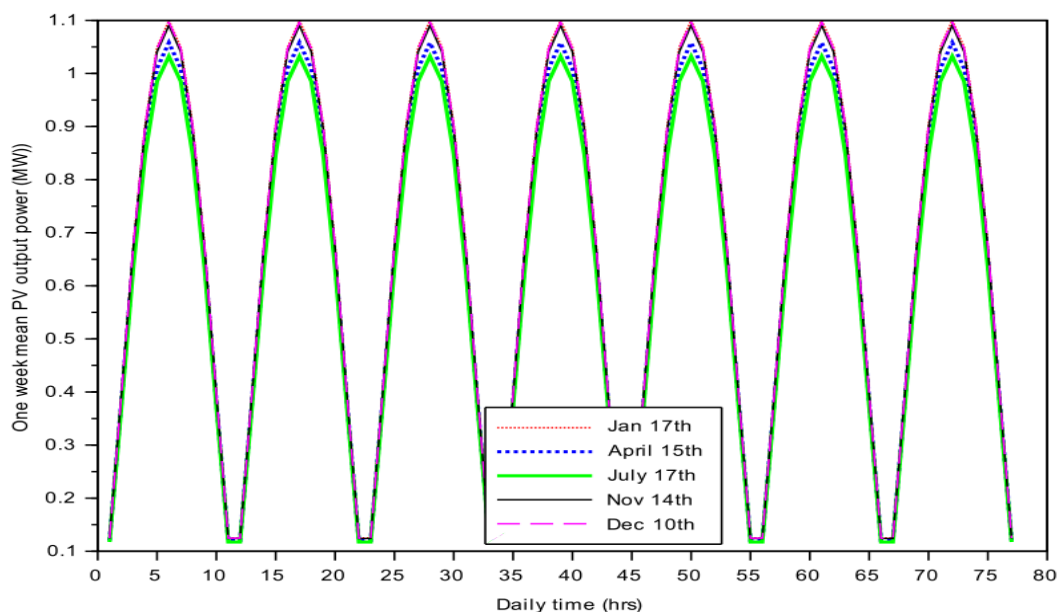


Figure 11: PV one week output power

Atmospheric transmittance, beam to diffuse transmission coefficient, clear sky normal radiation, horizontal beam radiation, diffuse to extraterrestrial beam radiation ratio and daily clearness index were calculated for different days of the months and year considering the daylight hours. The atmospheric transmittance was found to be increasing towards noon period daily from the morning period. Also, for the annual consideration, it has its peak around April and September. The extraterrestrial radiation, the clear sky normal radiation, the horizontal beam radiation, extraterrestrial horizontal radiation had their peak around the noon period daily as they gradually increase from morning period. The extraterrestrial radiation has its peak of 1413W/m^2 around the beginning and the end of the year period. The minimum value (1322W/m^2) was equally observed around the middle of the year due to the heavy rainy season and other factors witnessed during the period. It was also found that the clear sky normal beam radiation is always the highest radiation experienced throughout the year, this is followed by the clear sky horizontal radiation while the standard clear day radiation is the least among these three main sky radiations. The horizontal clear sky radiation has its peak value of 790W/m^2 around the midday hour but it maintains almost relatively higher value around the early and later part of the year but lower within the middle of the year through gradual decrease. The standard clear day radiation recorded its maximum value of 113.8W/m^2 during the dry season of the year and as well its minimum value of 106.5W/m^2 was observed during the middle of the year as rainy season is witness during the period. In the middle of the year (on the month of June), the major sky radiations and the transmittance are at their least value due to heavy rainy season witnessed during this period. September and April usually have the peak

atmospheric transmittance and clear sky index with the least value of the diffuse to extraterrestrial radiation ratio as the seasonal transition takes place during this period. Similarly, January and December have the peak value of the standard clear day radiation and the diffuse to extraterrestrial radiation ratio. On the aspect of power output, it can be observed that the approximate peak energetic and exergetic power value of 1.1MW and 0.55MW respectively. It can equally be observed that January, December and November period recorded the peak value of power based on the selected days for the simulation. And the same trend was maintained for the case of energetic and exergetic efficiencies with the respective peak efficiencies of 0.536% and 0.261% in the month of January.

References

1. R. Perez, P. Ineichen, R. Seals, s. J. Michal, R. Stewart, "Modeling daylight availability and irradiance components from direct and global irradiance, solar energy," *Renewable Energy*, 19 (2019) 40-44.
2. M. J. Ahmad and G. N. Tiwari, "Solar radiation models: a review," *International Journal of Energy Research*, 35(4) (2011) 270-290.
3. Y. Q. Tian, C. R. J. Davies, P. Gong, and B. W. Thorold, "Estimating solar radiation on slopes of arbitrary aspect," *Renewable Energy*, 109 (2001) 67-77.
4. L. Zalewski, A. Joulin, Y. Dutil, and D. Rouse, "Experimental study of small-scale solar wall," *Energy and Buildings*, 4(4) (2012) 1-19.
5. H. O. Menges, C. Ertekin, and M. H. Sonmete, "Evaluation of global solar radiation models for Konya, turkey," *Energy Conversion and Management*, 47 (2006) 3149-3173.
6. J. Glover and J. S. C. McCulloch, "The empirical relation between solar radiation and hours of sunshine," *Quarterly Journal of the Royal Meteorological Society*, 4(4) (1958) 172-175.
7. B. Ismail, D. Zied, and S. A. Mohamed, "Estimation of solar radiation on horizontal and inclined surfaces in sfax, tunisia," *Solar Energy conference, Tunisia*, 31 (2012) pp 4-12.
8. W. Lucien, "Basics in solar radiation at earth surface," *Quarterly Journal of the Royal Meteorological Society*, 38(4) (2018) 20-29, Edition 1, HAL Id: hal-01 676 634; https://hal-mines-paristech.archives-ouvertes.fr/hal-01_676_634
9. A. Seyed, M. Mousavi, H. Hizam, and G. Chandima, "Estimation of hourly, daily and monthly global solar radiation on inclined surfaces: Models re-visited," *Energies*, 10(134) (2017) 1-28.
10. K. D. Mohamad, "Solar radiation calculation," *Energies*, 5(40) (2017) 4-16.
11. A. K. Katiyar and C. K. Pandey, "A review of solar radiation models," *Journal of Renewable Energy*, 2013(8) (2013)1-12.
12. M. Diez-Mediavilla, D.A. Miguel, J. Bilbao, Measurement and comparison of diffuse solar irradiance models on inclined surfaces in valladolid (spain), *Energy Convers. Manag*, 46 (2005) 2075-2092.
13. T. C. Chineke, J. I. Aina, and S. S. Jagtap, "Solar radiation data base for nigeria," *Discovery and innovation*, 11(3/4) (2017) 207-210.
14. H. Qusay, J. Marek, M. Muzher, S. Katarzyna, S. Katarzyna, and G. Janusz, "Off-grid photovoltaic systems as a solution for the ambient pollution avoidance and iraq's rural areas electrification," *E3S Web of Conferences 10* (2016) pp 1-5. DOI: [10.1051/e3sconf/20161000093](https://doi.org/10.1051/e3sconf/20161000093)
15. J. Abdulateefa, K. Sopiana, W. Kaderb, B. Baisb, R. Sirwana, B. Bakhtyara, and O. Saadatiana, "Tech-noeconomics analysis of a photovoltaic system to provide electricity for a household," *International J. Sust. Green Energy*, 4 (2014) 23-31.
16. O. I. Okoro and T. C. Madueme, "Solar energy: A necessary investment in a developing economy," *Nigerian Journal of Technology*, 23(1) (2004) 58-64.

17. S. Wenqiang, Z. Zuquan, W. Yanhui, "Thermal analysis of a thermal energy storage unit to enhance a workshop heating system driven by industrial residual water," *Energies*, 10(219) (2017) 1-19.
18. F. G. Akinboro, L. A. Adejumobi, and V. Makinde, "Solar energy installation in nigeria: observations, prospects, problems and solutions," *Transnational Journal of Science and Technology*, 2(4) (2016) 73-84.
19. A. Mellit, M. Benghaneim, M. Bendekhis, "Artificial neural network model for prediction solar radiation data: Application for sizing stand-alone photovoltaic power system," *Solar Engineering Journal*, 15 (2016) 1-5.
20. A. Guessoum, S. Boubkeur, and A. Maafi, "A global irradiation model using radial basis function neural network," WREC, UK, (1998) 332-336.
21. M. Mohandes, B. A. M. Kassas, S. Rehman, and T. O. Halawani, "Use of radial basis functions for estimating monthly mean daily solar radiation," *Solar Energy*, 68 (2000) 161-168.
22. K. S. S. Michanelides, and F. Tymoios, "Prediction of maximum solar radiation using artificial neural networks," Proc. of WREC VII, Germany, (2002) pp1-5.
23. S. E. I. PVDI, "Design and installation manual," New Society Publishers, 2007.
24. S. C. Bhattacharyya, "Design and installation manual," *Energ. Sust. Dev.*, 16 (2012) 1-13.
25. M. Khan and M. Iqbal, "Design and installation manual," *Renew. Energies*, 30 (2005) 57-65.
26. J.F. Manirakiza, C.U. Ogbuefi, P.A. Okoro, "Potential of solar and wind energy for large scale power generation in eastern region of rwanda," *Am. J. Engg. Res.*, 8 (2019) 135-140.
27. A. Chauhan and R. P. Saini, "Techno-economic optimization-based approach for energy management of a stand-alone integrated renewable energy system for remote areas of India," *Renewable and sustainable energy reviews*, 94(1) (2016) 138-156.
28. S. Upadhyay and M. P. Sharma, "Development of hybrid energy system with cycle charging strategy using particle swarm optimization for a remote area in India," *Renewable and sustainable energy reviews*, 77 (2015) 586-598.
29. S. Rajanna and R. P. Saini, "Modeling of integrated renewable energy system for electrification of a remote area in India," *Renewable and sustainable energy reviews*, 90 (2016) 175-187
30. A. M. Romero and E. Zarza, "Concentrating solar thermal power," *Handbook of energy efficiency and renewable energy*, 21 (2007) 670-1208.
31. S. H. Muller and F. Trieb, "review of the technology, ingenia inform qr acad eng," *Handbook of energy efficiency and renewable energy*, 18 (2004) 43-50.
32. H. L. Zhang, J. Baeyens, J. Degreve, and G. Caceres, "Concentrated solar power plants: Review and design methodology," *Renewable and Sustainable Energy Reviews*, 22 (2013) 466-48.
- 33 K. IKHLEF and S. LARBI, "Simulation of electricity production by a solar tower power plant with thermal storage system in Algeria," *Int. J. Control, Energy & Elect. Engg.*, 8 (2019) 7-10.
34. T. Stephen, "The effect of electric load profiles on the performance of off-grid residential hybrid renewable energy systems," *Energies*, 8 (2015) 11, 120-11, 138, [doi:10.3390/en81011120](https://doi.org/10.3390/en81011120)
35. A. M. Patel and S. K. Singal, "Off grid rural electrification using integrated renewable energy system," (2016) 1-5.
36. K. B. Wahidul, M. Diesendorf, and P. Bryce, "Can photovoltaic technologies help attain sustainable rural development in bangladesh," *Energy policy*, 32 (2004) 1199-1207.
37. M. I. Fahmi, R. R. Kumar, R. Arelhi, and D. Isa, "Solar pv system for off-grid electrification in rural area," (2014) 1-6.
38. S. K. Nnadi and H. G. Ranjan, "A wind-pv-battery hybrid power system at sitakunda in bangladesh," *Energy policy*, 37 (2009) 3659-3664.

39. S. Islam and M. Marufa, "Rural electrification using pv: the success story of bangladesh," *Energy Procedia*, 23 (2013) 343-354.
40. ADP, Agricultural Development Programme, Ebonyi State chapter, 2015.
41. B. Y. H. Liu and R. C. Jordan, "Daily insolation on surfaces tilted toward the equator," *ASHRAE J.*, 3(10) (1962) 53-59.
42. T. Markvart, "Solar electricity," Chichester: 2nd edition, Wiley, 2000.
43. A. D. John and A. B. William, "Solar engineering of thermal processes," Solar Energy Laboratory, University of Wisconsin-Madison, 2nd edition, John Wiley & Sons, Inc., Hoboken, New Jersey, 2013.
44. B. Adrian, "Advanced engineering thermodynamics," 3rd edition, John Wiley and Sons, Inc., New Jersey., 2006.
45. O. N. Howard, E. A. Boniface, and O. O. Samuel, "A numerical study to predict the energy and exergy performances of a salinity gradient solar pond with thermal extraction," *Solar Energy*, 157 (2017) 744-761.

(2020) ; <http://www.jmaterenvironsci.com>